

J/ψ Suppression at Forward Rapidity in Pb-Pb Collisions at $\sqrt{s_{NN}} = 2.76$ TeVB. Abelev *et al.**

(ALICE Collaboration)

(Received 8 February 2012; published 16 August 2012)

The ALICE experiment has measured the inclusive J/ψ production in Pb-Pb collisions at $\sqrt{s_{NN}} = 2.76$ TeV down to zero transverse momentum in the rapidity range $2.5 < y < 4$. A suppression of the inclusive J/ψ yield in Pb-Pb is observed with respect to the one measured in pp collisions scaled by the number of binary nucleon-nucleon collisions. The nuclear modification factor, integrated over the 0%–80% most central collisions, is $0.545 \pm 0.032(\text{stat}) \pm 0.083(\text{syst})$ and does not exhibit a significant dependence on the collision centrality. These features appear significantly different from measurements at lower collision energies. Models including J/ψ production from charm quarks in a deconfined partonic phase can describe our data.

DOI: [10.1103/PhysRevLett.109.072301](https://doi.org/10.1103/PhysRevLett.109.072301)

PACS numbers: 25.75.Cj, 25.75.Dw, 25.75.Nq

Ultrarelativistic collisions of heavy nuclei aim at producing nuclear matter at high temperature and pressure. Under such conditions quantum chromodynamics predicts the existence of a deconfined state of partonic matter, the quark-gluon plasma (QGP). Among the possible probes of the QGP, heavy quarks are of particular interest since they are expected to be produced in the primary partonic scatterings and to coexist with the surrounding medium. Therefore, the measurement of quarkonium states and hadrons with open heavy flavor is expected to provide essential information on the properties of the strongly-interacting system formed in the early stages of heavy-ion collisions [1]. In particular, according to the color-screening model [2], measuring the in-medium dissociation probability of the different quarkonium states is expected to provide an estimate of the initial temperature of the system. In the past two decades, J/ψ production in heavy-ion collisions was intensively studied at the Super Proton Synchrotron (SPS) and at the Relativistic Heavy-Ion Collider (RHIC), from approximately 20 to 200 GeV center-of-mass energy per nucleon pair ($\sqrt{s_{NN}}$). At the SPS, a strong J/ψ suppression was found in the most central Pb-Pb collisions [3]. The observed suppression is larger than the one expected from Cold Nuclear Matter (CNM) effects, which include nuclear absorption and (anti-) shadowing. The dissociation of excited $c\bar{c}$ states like χ_c and $\psi(2S)$, which in pp collisions constitute about 40% of the inclusive J/ψ yield [1], is one possible interpretation of the observed suppression. A J/ψ suppression was also observed at RHIC, in central Au-Au collisions [4,5], at a level similar to the one observed at the SPS when

measured at midrapidity although it is larger at forward rapidity. Several models [6–9] attempt to reproduce the RHIC data by adding to the direct J/ψ production a regeneration component from deconfined charm quarks in the medium, which counteracts the J/ψ dissociation in a QGP. A quantitative description of these final-state effects is however difficult at the present time because of the lack of precision in the CNM effects and in the open charm cross section determination. The measurement of charmonium production is especially promising at the Large Hadron Collider (LHC) where the high energy density of the medium and the large number of $c\bar{c}$ pairs produced in central Pb-Pb collisions should help to disentangle between the different suppression and regeneration scenarios. At the LHC, a suppression of inclusive J/ψ with high transverse momentum was observed in central Pb-Pb collisions at $\sqrt{s_{NN}} = 2.76$ TeV with respect to peripheral collisions or pp collisions at the same energy by ATLAS [10] and CMS [11], respectively.

In this Letter, we report ALICE results on inclusive J/ψ production in Pb-Pb collisions at $\sqrt{s_{NN}} = 2.76$ TeV at forward rapidity, measured via the $\mu^+\mu^-$ decay channel. Our measurement encloses the low transverse momentum region that is not accessible to other LHC experiments and thus complements their observations. The J/ψ corrected yield in Pb-Pb collisions is combined with the one measured in pp collisions at the same center-of-mass energy [12] to form the J/ψ nuclear modification factor R_{AA} . The results are presented as a function of collision centrality and rapidity (y), and in intervals of transverse momentum (p_t).

The ALICE detector is described in [13]. At forward rapidity ($2.5 < y < 4$) the production of quarkonium states is measured in the muon spectrometer [14] down to $p_t = 0$. The spectrometer consists of a ten interaction length thick absorber filtering the muons in front of five tracking stations comprising two planes of cathode pad chambers each, with the third station inside a dipole magnet with a

*Full author list given at the end of the article.

3 Tm field integral. The tracking apparatus is completed by a triggering system made of four planes of resistive plate chambers downstream of a 1.2 m thick iron wall, which absorbs secondary hadrons escaping from the front absorber and low momentum muons coming mainly from π and K decays. In addition, the silicon pixel detector (SPD) and scintillator arrays (VZERO) were used in this analysis. The VZERO counters, two arrays of 32 scintillator tiles each, cover $2.8 \leq \eta \leq 5.1$ (VZERO-A) and $-3.7 \leq \eta \leq -1.7$ (VZERO-C). The SPD consists of two cylindrical layers covering $|\eta| \leq 2.0$ and $|\eta| \leq 1.4$ for the inner and outer layers, respectively. All these detectors have full azimuthal coverage. The minimum bias (MB) trigger requirement used for this analysis consists of a logical AND of the three following conditions: (i) a signal in two readout chips in the outer layer of the SPD, (ii) a signal in VZERO-A, (iii) a signal in VZERO-C, providing a high triggering efficiency for hadronic interactions. The beam induced background was further reduced by timing cuts on the signals from the VZERO and from the zero degree calorimeters (ZDC). The contribution from electromagnetic processes was removed with a cut on the energy deposited in the neutron ZDCs. The centrality determination is based on a fit of the VZERO amplitude distribution as described in [15]. A cut corresponding to the most central 80% of the nuclear cross section was applied; for these events the MB trigger is fully efficient. A data sample of 17.7×10^6 Pb-Pb collisions collected in 2010 satisfying all the above conditions is used in the following analysis. It corresponds to an integrated luminosity $\mathcal{L}_{\text{int}} \approx 2.9 \mu\text{b}^{-1}$. This data sample was further divided into five centrality classes from 0%–10% (central collisions) to 50%–80% (peripheral collisions).

J/ψ candidates are formed by combining pairs of opposite-sign (OS) tracks reconstructed in the geometrical acceptance of the muon spectrometer. To reduce the combinatorial background, the reconstructed tracks in the muon tracking chambers are required to match a track segment in the muon trigger system. The resulting invariant mass distribution of OS muon pairs for the 0%–80% most central Pb-Pb collisions is shown in Fig. 1, where a J/ψ signal above the combinatorial background is clearly visible. The J/ψ raw yield was extracted by using two different methods. The OS dimuon invariant mass distribution was fitted with a Crystal Ball (CB) function to reproduce the J/ψ line shape, and a sum of two exponentials to describe the underlying continuum. The CB function connects a Gaussian core with a power-law tail [16] at low mass to account for energy loss fluctuations and radiative decays. At high transverse momenta ($p_t \geq 3 \text{ GeV}/c$), the sum of two exponentials does not describe correctly the underlying continuum; it was replaced by a third order polynomial. Alternatively, the combinatorial background was subtracted using an event-mixing technique. The resulting mass distribution was fitted with

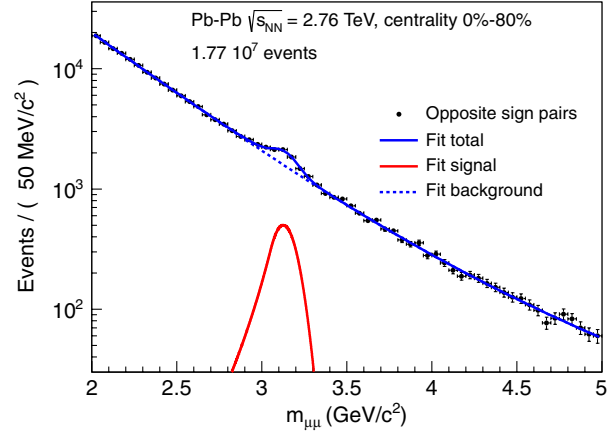


FIG. 1 (color online). Invariant mass spectrum of $\mu^+ \mu^-$ pairs (solid black circles) with $p_t \geq 0$ and $2.5 < y < 4$ in the 0%–80% most central Pb-Pb collisions.

a CB function and an exponential or a first order polynomial to describe the remaining background. The event-mixing was preferred to the like-sign subtraction technique since it is less sensitive to correlated signal pairs present in the like-sign spectra and gives better statistical precision. The $\psi(2S)$ was not included in the signal line shape since its contribution is negligible. The width of the J/ψ mass peak depends on the resolution of the spectrometer which can be affected by the detector occupancy that increases with centrality. This effect, evaluated by embedding simulated $J/\psi \rightarrow \mu^+ \mu^-$ decays into real events, was found to be less than 2%. This conclusion was confirmed by a direct measurement of the tracking chamber resolution versus centrality using reconstructed tracks. Therefore, the same CB line shape can be used for all centrality classes. The parameters of the CB tails were fixed to the values obtained either in simulations or in pp collisions where the signal to background ratio is much higher. For each of these choices, the mean and width of the CB Gaussian part were fixed to the value obtained by fitting the mass distribution in the centrality range 0%–80%. In addition, a variation of the width of ± 1 standard deviation was applied to account for uncertainties (varying the mean has turned out to have a negligible effect in comparison). The raw J/ψ yield in each centrality class was determined as the average of the results obtained with the two fitting approaches and the various CB parametrizations, while the corresponding systematic uncertainties were defined as the RMS of these results. It was also checked that every individual result differs from the mean value by less than three RMS. The raw J/ψ yield in our Pb-Pb sample is $2350 \pm 139(\text{stat}) \pm 189(\text{syst})$. The invariant mass resolution is around $78 \text{ MeV}/c^2$, in very good agreement with the embedded J/ψ simulations. The signal to background ratio integrated over $\pm 3\sigma$ of the mass resolution varies from 0.1 for central collisions to 1.5 for peripheral collisions.

The measured number of J/ψ ($N_{J/\psi}^i$) was normalized to the number of events in the corresponding centrality class (N_{events}^i) and further corrected for the branching ratio (BR) of the dimuon decay channel, the acceptance A and the efficiency ϵ^i of the detector. The inclusive J/ψ yield in each centrality class i for our measured p_t and y ranges ($\Delta p_t, \Delta y$) is then given by:

$$Y_{J/\psi}^i(\Delta p_t, \Delta y) = \frac{N_{J/\psi}^i}{\text{BR}_{J/\psi \rightarrow \mu^+ \mu^-} N_{\text{events}}^i A \epsilon^i}. \quad (1)$$

The product $A\epsilon$ was determined from Monte Carlo simulations. The generated J/ψ p_t and y distributions were extrapolated from existing measurements [17], including shadowing effects from EKS98 calculations [18]. As the measured J/ψ polarization in pp collisions at $\sqrt{s} = 7$ TeV is compatible with zero [19], and J/ψ mesons produced from charm quarks in the medium are expected to be unpolarized, we presume J/ψ production is unpolarized. For the tracking chambers, the time-dependent status of each electronic channel during the data taking period was taken into account as well as the residual misalignment of the detection elements. The efficiencies of the muon trigger chambers were determined from data and were then applied in the simulations [20]. Finally, the dependence of the efficiency on the detector occupancy was included using the embedding technique. For J/ψ mesons emitted at $2.5 < y < 4$ and $p_t \geq 0$, a run-averaged value of $A\epsilon = 0.176$ with a 8% relative systematic uncertainty was obtained. A $8\% \pm 2\%$ (syst) relative decrease of the efficiency was observed when going from peripheral to central collisions.

The J/ψ yield measured in Pb-Pb collisions in centrality class i is combined with the inclusive J/ψ cross section measured in pp collisions at the same energy to form the nuclear modification factor R_{AA} defined as:

$$R_{AA}^i = \frac{Y_{J/\psi}^i(\Delta p_t, \Delta y)}{\langle T_{AA}^i \rangle \sigma_{J/\psi}^{pp}(\Delta p_t, \Delta y)}. \quad (2)$$

The inclusive J/ψ cross section in pp collisions $\sigma_{J/\psi}^{pp}(\Delta p_t, \Delta y)$ was measured using the same apparatus and analysis technique within the corresponding p_t and y range [12]. The reference value $\sigma_{J/\psi}^{pp}$ used for the calculation of R_{AA} integrated over p_t and y is $3.34 \pm 0.13(\text{stat}) \pm 0.24(\text{syst}) \pm 0.12(\text{lumi})_{-1.07}^{+0.53}(\text{pol}) \mu\text{b}$. The centrality intervals used in this analysis, the average number of participating nucleons $\langle N_{\text{part}} \rangle$ and average value of the nuclear overlap function $\langle T_{AA} \rangle$ derived from a Glauber model calculation [15] are summarized in Table I. Since our most peripheral bin is rather large, the variables $\langle N_{\text{part}}^w \rangle$ and the charged-particle density measured at midrapidity $dN_{\text{ch}}^w/d\eta|_{\eta=0}$ were weighted by the number of binary collisions $\langle N_{\text{coll}} \rangle$. Indeed in absence of nuclear matter effects, the J/ψ production cross section in nucleus-nucleus collisions is expected to scale with $\langle N_{\text{coll}} \rangle$.

TABLE I. The average number of participating nucleons $\langle N_{\text{part}} \rangle$ without and with $\langle N_{\text{coll}} \rangle$ weighting, the midrapidity charged-particle density $dN_{\text{ch}}^w/d\eta|_{\eta=0}$ with $\langle N_{\text{coll}} \rangle$ weighting and the average value of the nuclear overlap function $\langle T_{AA} \rangle$ for the centrality classes expressed in percentages of the nuclear cross section [15].

Centrality	$\langle N_{\text{part}} \rangle$	$\langle N_{\text{part}}^w \rangle$	$\frac{dN_{\text{ch}}^w}{d\eta _{\eta=0}}$	$\langle T_{AA} \rangle$ (mb $^{-1}$)
0%–10%	356 ± 4	361 ± 4	1463 ± 60	23.5 ± 1.0
10%–20%	260 ± 4	264 ± 4	979 ± 37	14.4 ± 0.6
20%–30%	186 ± 4	189 ± 4	658 ± 23	8.74 ± 0.37
30%–50%	107 ± 3	117 ± 3	369 ± 13	3.87 ± 0.18
50%–80%	32 ± 2	47 ± 2	110 ± 5	0.72 ± 0.05
0%–80%	139 ± 3	264 ± 4	–	7.03 ± 0.27

The weighted values are given in Table I and are used for the ALICE data points in the following figures. All systematic uncertainties entering the R_{AA} calculation are listed in Table II. In the figures below, the point to point uncorrelated systematic uncertainties are represented as boxes at the position of the data points while the statistical ones are indicated by vertical bars. Correlated systematic uncertainties are quoted directly on the figures.

The inclusive J/ψ R_{AA} measured by ALICE at $\sqrt{s_{NN}} = 2.76$ TeV in the range $2.5 < y < 4$ and $p_t \geq 0$ is shown in Fig. 2 as a function of $dN_{\text{ch}}/d\eta|_{\eta=0}$ (left) and N_{part} (right). The charged-particle density closely relates to the energy density of the created medium whereas the number of participants reflects the collision geometry. The centrality integrated J/ψ R_{AA} is $R_{AA}^{0\%-80\%} = 0.545 \pm 0.032(\text{stat}) \pm 0.083(\text{syst})$, indicating a clear J/ψ suppression. The contribution from beauty hadron feed-down to the inclusive J/ψ yield in our y and p_t domain was measured by the LHCb collaboration to be about 10% in pp collisions at $\sqrt{s} = 7$ TeV [21]. Therefore, the difference between the prompt J/ψ R_{AA} and our inclusive measurement is expected not to exceed 11% if N_{coll} scaling of beauty production is assumed and shadowing effects are neglected. All R_{AA} results are presented assuming unpolarized J/ψ production in pp and Pb-Pb collisions. The comparison

TABLE II. Summary of the systematic uncertainties entering the R_{AA} calculation. The type I (II) stands for correlated (uncorrelated) uncertainties. The centrality dependence for the type II is given as a range.

Source	Value	Type
signal extraction	5%–12%	II
input MC parametrization	5%	I
tracking efficiency	5% and 0%–1%	I and II
trigger efficiency	4% and 0%–2%	I and II
matching efficiency	2%	I
T_{AA}	4%–8%	II
$\sigma_{J/\psi}^{pp}$ at $\sqrt{s_{NN}} = 2.76$ TeV	9%	I

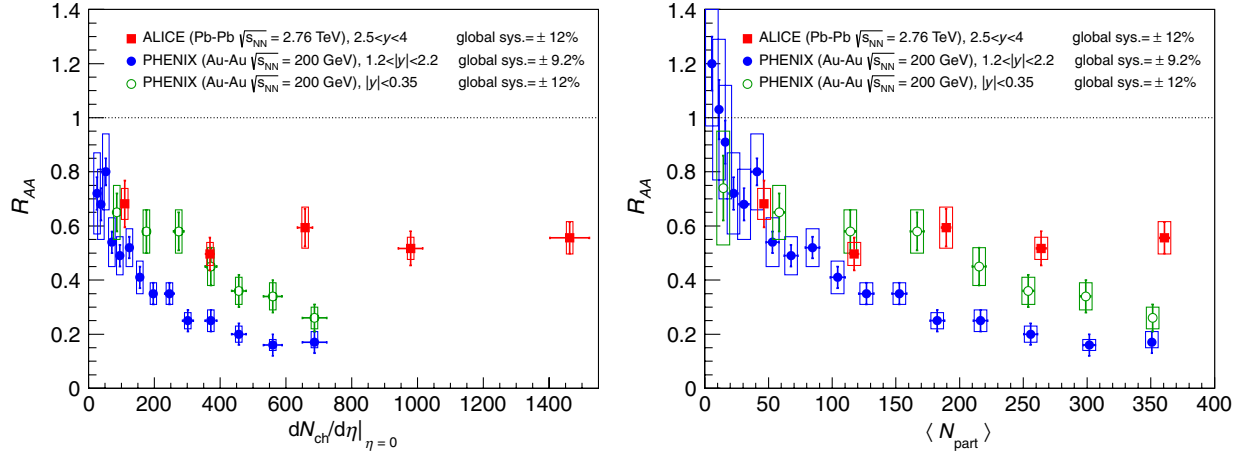


FIG. 2 (color online). Inclusive J/ψ R_{AA} as a function of the midrapidity charged-particle density (left) and the number of participating nucleons (right) measured in Pb-Pb collisions at $\sqrt{s_{NN}} = 2.76$ TeV compared to PHENIX results in Au-Au collisions at $\sqrt{s_{NN}} = 200$ GeV at midrapidity and forward rapidity [4,5,23]. The ALICE data points are placed at the $dN_{ch}^w/d\eta|_{\eta=0}$ and $\langle N_{part}^w \rangle$ values defined in Table I.

with the PHENIX measurements [22] at $\sqrt{s_{NN}} = 200$ GeV at forward rapidity $1.2 < |y| < 2.2$ [5,23] shows that our inclusive J/ψ R_{AA} is almost a factor of 3 larger for $dN_{ch}/d\eta|_{\eta=0} \gtrsim 600$ ($N_{part} \gtrsim 180$). In addition, our results do not exhibit a significant centrality dependence.

The rapidity dependence of the J/ψ R_{AA} is presented in Fig. 3 for two p_t domains, $p_t \geq 0$ and $p_t \geq 3$ GeV/c. The J/ψ reference cross sections in pp collisions [24] and the R_{AA} total systematic uncertainties, indicated as open boxes in the figure, were evaluated in the same kinematic range. Our results are shown together with a measurement from CMS [11] of the inclusive J/ψ R_{AA} in the rapidity range $1.6 < |y| < 2.4$ with $p_t \geq 3$ GeV/c. No significant

rapidity dependence can be seen in the J/ψ R_{AA} for $p_t \geq 0$. For $p_t \geq 3$ GeV/c, a decrease of R_{AA} is observed with increasing rapidity reaching a value of $0.289 \pm 0.061(\text{stat}) \pm 0.078(\text{syst})$ for $3.25 < y < 4$. At LHC energies, J/ψ nuclear absorption is likely to be negligible and the modification of the gluon distribution function is dominated by shadowing effects [25]. An estimate of shadowing effects is shown in Fig. 3 within the color singlet model at leading order [26] and the color evaporation model at next to leading order [27]. The shadowing is, respectively, calculated with the nDSg and the EPS09 parametrizations [27] of the nuclear parton distribution function (nPDF). For nDSg (EPS09) the upper and lower limits correspond to the uncertainty in the factorization scale (uncertainty of the nPDF). The effect of shadowing shows no dependence with rapidity and its overall amount is reduced by the addition of a transverse momentum cut. At most, shadowing effects are expected to lower the R_{AA} from 1 to 0.7. Recent color glass condensate (CGC) calculations for LHC energies may indicate a larger initial state suppression ($R_{AA} \approx 0.5$) [28]. However, any J/ψ suppression due to initial state effects, CGC or shadowing, will be stronger at lower p_t contrary to the data behavior.

In Fig. 4, our measurement is compared with theoretical models that include a J/ψ regeneration component from deconfined charm quarks in the medium. The statistical hadronization model [6,29] assumes deconfinement and a thermal equilibration of the bulk of the $c\bar{c}$ pairs. Then charmonium production occurs only at phase boundary by statistical hadronization of charm quarks. The prediction is given for two values of $d\sigma_{c\bar{c}}/dy$ in absence of a measurement for Pb-Pb collisions. The two transport model results [30,31] presented in the same figure differ mostly in the rate equation controlling the J/ψ dissociation and regeneration. Both are shown as a band which connects the results obtained with (lower limit) and

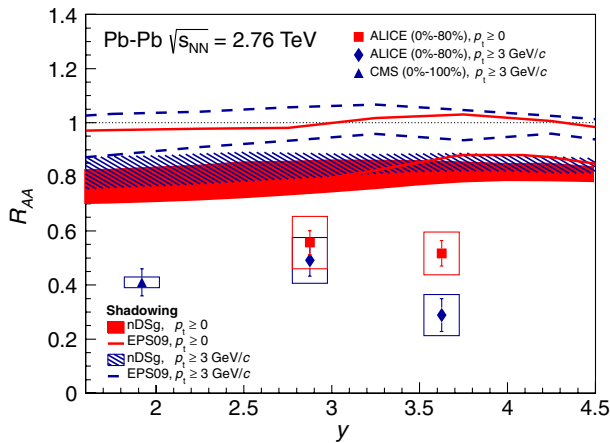


FIG. 3 (color online). Centrality integrated inclusive J/ψ R_{AA} measured in Pb-Pb collisions at $\sqrt{s_{NN}} = 2.76$ TeV as a function of rapidity for two p_t ranges. The open boxes contain the total systematic uncertainties except the ones on the integrated luminosity in the pp reference and on the T_{AA} , i.e., 5.2% (8.3%) for the ALICE (CMS [11]) data. The two models [26,27] predict the R_{AA} due only to shadowing effects for nDSg (shaded areas) and EPS09 (lines) nPDF, respectively.

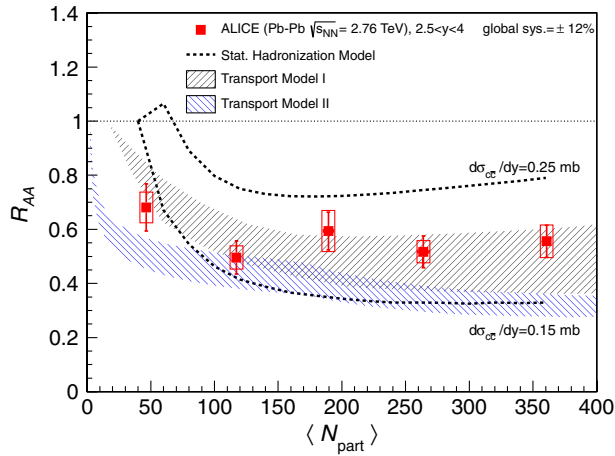


FIG. 4 (color online). Inclusive J/ψ R_{AA} measured in Pb-Pb collisions at $\sqrt{s_{NN}} = 2.76$ TeV compared to the predictions by Statistical Hadronization model [29], Transport model I [30] and II [31], see text for details. The ALICE data points are placed at the $\langle N_{part}^w \rangle$ values defined in Table I.

without (higher limit) shadowing. The width of the band can be interpreted as the uncertainty of the prediction. In both transport models, the amount of regenerated J/ψ in the most central collisions contributes to about 50% of the production yield, the rest being from initial production.

In summary, we have presented the first measurement of inclusive J/ψ nuclear modification factor down to $p_t = 0$ at forward rapidity in Pb-Pb collisions at $\sqrt{s_{NN}} = 2.76$ TeV. The J/ψ R_{AA} is larger than the one measured at the SPS and at RHIC for most central collisions and does not exhibit a significant centrality dependence. Statistical hadronization and transport models which, respectively, feature a full and a partial J/ψ production from charm quarks in the QGP phase can describe the data. Towards a definitive conclusion about the role of J/ψ production from deconfined charm quarks in a partonic phase, the amount of shadowing needs to be measured precisely in pPb collisions. In this context, the measurement of open charm and J/ψ elliptic flow will also help to determine the degree of thermalization for charm quarks.

The ALICE collaboration would like to thank all its engineers and technicians for their invaluable contributions to the construction of the experiment and the CERN accelerator teams for the outstanding performance of the LHC complex. The ALICE collaboration acknowledges the following funding agencies for their support in building and running the ALICE detector: Calouste Gulbenkian Foundation from Lisbon and Swiss Fonds Kidagan, Armenia; Conselho Nacional de Desenvolvimento Científico e Tecnológico (CNPq), Financiadora de Estudos e Projetos (FINEP), Fundação de Amparo à Pesquisa do Estado de São Paulo (FAPESP); National Natural Science Foundation of China (NSFC), the Chinese Ministry of Education (CMOE) and the Ministry of Science and Technology of China (MSTC); Ministry of

Education and Youth of the Czech Republic; Danish Natural Science Research Council, the Carlsberg Foundation and the Danish National Research Foundation; The European Research Council under the European Community's Seventh Framework Programme; Helsinki Institute of Physics and the Academy of Finland; French CNRS-IN2P3, the "Region Pays de Loire", "Region Alsace", "Region Auvergne" and CEA, France; German BMBF and the Helmholtz Association; General Secretariat for Research and Technology, Ministry of Development, Greece; Hungarian OTKA and National Office for Research and Technology (NKTH); Department of Atomic Energy and Department of Science and Technology of the Government of India; Istituto Nazionale di Fisica Nucleare (INFN) of Italy; MEXT Grant-in-Aid for Specially Promoted Research, Japan; Joint Institute for Nuclear Research, Dubna; National Research Foundation of Korea (NRF); CONACYT, DGAPA, México, ALFA-EC and the HELEN Program (High-Energy physics Latin-American-European Network); Stichting voor Fundamenteel Onderzoek der Materie (FOM) and the Nederlandse Organisatie voor Wetenschappelijk Onderzoek (NWO), Netherlands; Research Council of Norway (NFR); Polish Ministry of Science and Higher Education; National Authority for Scientific Research-NASR (Autoritatea Națională pentru Cercetare Științifică-ANCS); Federal Agency of Science of the Ministry of Education and Science of Russian Federation, International Science and Technology Center, Russian Academy of Sciences, Russian Federal Agency of Atomic Energy, Russian Federal Agency for Science and Innovations and CERN-INTAS; Ministry of Education of Slovakia; Department of Science and Technology, South Africa; CIEMAT, EELA, Ministerio de Educación y Ciencia of Spain, Xunta de Galicia (Consellería de Educación), CEADEN, Cubaenergía, Cuba, and IAEA (International Atomic Energy Agency); Swedish Research Council (VR) and Knut & Alice Wallenberg Foundation (KAW); Ukraine Ministry of Education and Science; United Kingdom Science and Technology Facilities Council (STFC); The United States Department of Energy, the United States National Science Foundation, the State of Texas, and the State of Ohio.

-
- [1] M. Bedjidian, D. Blaschke, G. T. Bodwin, N. Carrer, and B. Cole *et al.*, [arXiv:hep-ph/0311048](https://arxiv.org/abs/hep-ph/0311048).
 - [2] T. Matsui and H. Satz, *Phys. Lett. B* **178**, 416 (1986).
 - [3] B. Alessandro *et al.* (NA50 Collaboration), *Eur. Phys. J. C* **39**, 335 (2005).
 - [4] A. Adare *et al.* (PHENIX Collaboration), *Phys. Rev. Lett.* **98**, 232301 (2007).
 - [5] A. Adare *et al.* (PHENIX Collaboration), *Phys. Rev. C* **84**, 054912 (2011).
 - [6] P. Braun-Munzinger and J. Stachel, *Phys. Lett. B* **490**, 196 (2000).

- [7] R. L. Thews, M. Schroedter, and J. Rafelski, *Phys. Rev. C* **63**, 054905 (2001).
- [8] A. Andronic, P. Braun-Munzinger, K. Redlich, and J. Stachel, *Phys. Lett. B* **652**, 259 (2007).
- [9] X. Zhao and R. Rapp, *Phys. Lett. B* **664**, 253 (2008).
- [10] G. Aad *et al.* (ATLAS Collaboration), *Phys. Lett. B* **697**, 294 (2011).
- [11] S. Chatrchyan *et al.* (CMS Collaboration), *J. High Energy Phys.* **05** (2012) 063.
- [12] B. Abelev *et al.* (ALICE Collaboration), [arXiv:1203.3641](https://arxiv.org/abs/1203.3641).
- [13] K. Aamodt *et al.* (ALICE Collaboration), *JINST* **3**, S08002 (2008).
- [14] In the ALICE reference frame, the muon spectrometer covers a negative η range and consequently a negative y range. We have chosen to present our results with a positive y notation.
- [15] K. Aamodt *et al.* (ALICE Collaboration), *Phys. Rev. Lett.* **106**, 032301 (2011).
- [16] J.E. Gaiser, Ph.D. thesis, Stanford 1982, appendix-F, SLAC-R-255.
- [17] F. Bossu, Z. del Valle, A. de Falco, M. Gagliardi, and S. Grigoryan *et al.*, [arXiv:1103.2394](https://arxiv.org/abs/1103.2394).
- [18] K. J. Eskola, V. J. Kolhinen, and C. A. Salgado, *Eur. Phys. J. C* **9**, 61 (1999).
- [19] B. Abelev *et al.* (ALICE Collaboration), *Phys. Rev. Lett.* **108**, 082001 (2012).
- [20] D. Stocco *et al.* (ALICE Collaboration), Report No. ALICE-INT-2008-004, 2008.
- [21] R. Aaij *et al.* (LHCb Collaboration), *Eur. Phys. J. C* **71**, 1645 (2011).
- [22] The PHENIX midrapidity J/ψ R_{AA} was measured in centrality classes wider than the ones in which the midrapidity charged-particle density is given [23] Therefore a linear interpolation was done to extract the midrapidity charged-particle density in the three most peripheral classes.
- [23] S. S. Adler *et al.* (PHENIX Collaboration), *Phys. Rev. C* **71**, 049901 (2005).
- [24] We report here $\sigma_{J/\psi}^{pp}(p_t \geq 3 \text{ GeV}/c, 2.5 < y \leq 3.25) = 0.34 \pm 0.03(\text{stat}) \pm 0.03(\text{syst}) \pm 0.02(\text{lumi}) \mu\text{b}$ and $\sigma_{J/\psi}^{pp}(p_t \geq 3 \text{ GeV}/c, 3.25 < y < 4) = 0.50 \pm 0.04(\text{stat}) \pm 0.04(\text{syst}) \pm 0.02(\text{lumi}) \mu\text{b}$ that cannot directly be extracted from [12].
- [25] C. Lourenço, R. Vogt, and H. K. Wöhri, *J. High Energy Phys.* **02** (2009) 014.
- [26] E. Ferreira, F. Fleuret, J. Lansberg, N. Matagne, and A. Rakotozafindrabe, *Nucl. Phys. A* **855**, 327 (2011); (private communication).
- [27] R. Vogt, *Phys. Rev. C* **81**, 044903 (2010); (private communication).
- [28] F. Dominguez, D. Kharzeev, E. Levin, A. Mueller, and K. Tuchin, *Phys. Lett. B* **710**, 182 (2012).
- [29] A. Andronic, P. Braun-Munzinger, K. Redlich, and J. Stachel, *J. Phys. G* **38**, 124081 (2011).
- [30] X. Zhao and R. Rapp, *Nucl. Phys. A* **859**, 114 (2011).
- [31] Y.-P. Liu, Z. Qu, N. Xu, and P.-F. Zhuang, *Phys. Lett. B* **678**, 72 (2009); (private communication).

B. Abelev,¹ J. Adam,² D. Adamová,³ A. M. Adare,⁴ M. M. Aggarwal,⁵ G. Aglieri Rinella,⁶ A. G. Agocs,⁷ A. Agostinelli,⁸ S. Aguilar Salazar,⁹ Z. Ahammed,¹⁰ A. Ahmad Masoodi,¹¹ N. Ahmad,¹¹ S. U. Ahn,^{12,13} A. Akindinov,¹⁴ D. Aleksandrov,¹⁵ B. Alessandro,¹⁶ R. Alfaro Molina,⁹ A. Alici,^{17,18} A. Alkin,¹⁹ E. Almaráz Aviña,⁹ J. Alme,²⁰ T. Alt,²¹ V. Altini,²² S. Altinpinar,²³ I. Altsybeev,²⁴ C. Andrei,²⁵ A. Andronic,²⁶ V. Anguelov,²⁷ J. Anielski,²⁸ C. Anson,²⁹ T. Antičić,³⁰ F. Antinori,³¹ P. Antonioli,¹⁷ L. Aphecetche,³² H. Appelshäuser,³³ N. Arbor,³⁴ S. Arceci,⁸ A. Arend,³³ N. Armesto,³⁵ R. Arnaldi,¹⁶ T. Aronsson,⁴ I. C. Arsene,²⁶ M. Arslanok,³³ A. Asryan,²⁴ A. Augustinus,⁶ R. Averbeck,²⁶ T. C. Awes,³⁶ J. Äystö,³⁷ M. D. Azmi,¹¹ M. Bach,²¹ A. Badalà,³⁸ Y. W. Baek,^{12,13} R. Bailhache,³³ R. Bala,¹⁶ R. Baldini Ferroli,¹⁸ A. Baldisseri,³⁹ A. Baldit,¹² F. Baltasar Dos Santos Pedrosa,⁶ J. Bán,⁴⁰ R. C. Baral,⁴¹ R. Barbera,⁴² F. Barile,²² G. G. Barnaföldi,⁷ L. S. Barnby,⁴³ V. Barret,¹² J. Bartke,⁴⁴ M. Basile,⁸ N. Bastid,¹² B. Bathen,²⁸ G. Batigne,³² B. Batyunya,⁴⁵ C. Baumann,³³ I. G. Bearden,⁴⁶ H. Beck,³³ I. Belikov,⁴⁷ F. Bellini,⁸ R. Bellwied,⁴⁸ E. Belmont-Moreno,⁹ G. Bencedi,⁷ S. Beole,⁴⁹ I. Berceanu,²⁵ A. Bercuci,²⁵ Y. Berdnikov,⁵⁰ D. Berenyi,⁷ C. Bergmann,²⁸ D. Berzano,¹⁶ L. Betev,⁶ A. Bhasin,⁵¹ A. K. Bhati,⁵ L. Bianchi,⁴⁹ N. Bianchi,⁵² C. Bianchin,⁵³ J. Bielčik,² J. Bielčíková,³ A. Bilandžić,^{54,46} S. Bjelogrić,⁵⁵ F. Blanco,⁵⁶ F. Blanco,⁴⁸ D. Blau,¹⁵ C. Blume,³³ M. Boccioli,⁶ N. Bock,²⁹ A. Bogdanov,⁵⁷ H. Bøggild,⁴⁶ M. Bogolyubsky,⁵⁸ L. Boldizsár,⁷ M. Bombara,⁵⁹ J. Book,³³ H. Borel,³⁹ A. Borissov,⁶⁰ S. Bose,⁶¹ F. Bossú,⁴⁹ M. Botje,⁵⁴ S. Böttger,⁶² B. Boyer,⁶³ E. Braidot,⁶⁴ P. Braun-Munzinger,²⁶ M. Bregant,³² T. Breitner,⁶² T. A. Browning,⁶⁵ M. Broz,⁶⁶ R. Brun,⁶ E. Bruna,^{49,16} G. E. Bruno,²² D. Budnikov,⁶⁷ H. Buesching,³³ S. Bufalino,^{49,16} K. Bugaiev,¹⁹ O. Busch,²⁷ Z. Buthelezi,⁶⁸ D. Caballero Orduna,⁴ D. Caffarri,⁵³ X. Cai,⁶⁹ H. Caines,⁴ E. Calvo Villar,⁷⁰ P. Camerini,⁷¹ V. Canoa Roman,^{72,73} G. Cara Romeo,¹⁷ W. Carena,⁶ F. Carena,⁶ N. Carlin Filho,⁷⁴ F. Carminati,⁶ C. A. Carrillo Montoya,⁶ A. Casanova Díaz,⁵² J. Castillo Castellanos,³⁹ J. F. Castillo Hernandez,²⁶ E. A. R. Casula,⁷⁵ V. Catanescu,²⁵ C. Cavicchioli,⁶ J. Cepila,² P. Cerello,¹⁶ B. Chang,^{37,76} S. Chapeland,⁶ J. L. Charvet,³⁹ S. Chattopadhyay,¹⁰ S. Chattopadhyay,⁶¹ I. Chawla,⁵ M. Cherney,⁷⁷ C. Cheshkov,^{6,78} B. Cheynis,⁷⁸ E. Chiavassa,¹⁶ V. Chibante Barroso,⁶ D. D. Chinellato,⁷⁹ P. Chochula,⁶ M. Chojnacki,⁵⁵ P. Christakoglou,^{54,55} C. H. Christensen,⁴⁶ P. Christiansen,⁸⁰ T. Chujo,⁸¹ S. U. Chung,⁸² C. Cicalo,⁸³ L. Cifarelli,^{8,6} F. Cindolo,¹⁷ J. Cleymans,⁶⁸ F. Cocchetti,¹⁸ F. Colamaria,²² D. Colella,²² G. Conesa Balbastre,³⁴ Z. Conesa del Valle,⁶ P. Constantin,²⁷ G. Contin,⁷¹

- J. G. Contreras,⁷² T. M. Cormier,⁶⁰ Y. Corrales Morales,⁴⁹ P. Cortese,⁸⁴ I. Cortés Maldonado,⁷³ M. R. Cosentino,^{64,79} F. Costa,⁶ M. E. Cotallo,⁵⁶ E. Crescio,⁷² P. Crochet,¹² E. Cruz Alaniz,⁹ E. Cuautle,⁸⁵ L. Cunqueiro,⁵² A. Dainese,^{53,31} H. H. Dalsgaard,⁴⁶ A. Danu,⁸⁶ K. Das,⁶¹ I. Das,^{61,63} D. Das,⁶¹ A. Dash,⁷⁹ S. Dash,⁸⁷ S. De,¹⁰ G. O. V. de Barros,⁷⁴ A. De Caro,^{88,18} G. de Cataldo,⁸⁹ J. de Cuveland,²¹ A. De Falco,⁷⁵ D. De Gruttola,⁸⁸ H. Delagrangé,³² E. Del Castillo Sanchez,⁶ A. Deloff,⁹⁰ V. Demanov,⁶⁷ N. De Marco,¹⁶ E. Dénes,⁷ S. De Pasquale,⁸⁸ A. Deppman,⁷⁴ G. D'Erasmo,²² R. de Rooij,⁵⁵ M. A. Diaz Corchero,⁵⁶ D. Di Bari,²² T. Dietel,²⁸ C. Di Giglio,²² S. Di Liberto,⁹¹ A. Di Mauro,⁶ P. Di Nezza,⁵² R. Divià,⁶ Ø. Djuvsland,²³ A. Dobrin,^{60,80} T. Dobrowolski,⁹⁰ I. Domínguez,⁸⁵ B. Dönigus,²⁶ O. Dordic,⁹² O. Driga,³² A. K. Dubey,¹⁰ L. Ducroux,⁷⁸ P. Dupieux,¹² A. K. Dutta Majumdar,⁶¹ M. R. Dutta Majumdar,¹⁰ D. Elia,⁸⁹ D. Emschermann,²⁸ H. Engel,⁶² H. A. Erdal,²⁰ B. Espagnon,⁶³ M. Estienne,³² S. Esumi,⁸¹ D. Evans,⁴³ G. Eyyubova,⁹² D. Fabris,^{53,31} J. Faivre,³⁴ D. Falchieri,⁸ A. Fantoni,⁵² M. Fasel,²⁶ R. Fearick,⁶⁸ A. Fedunov,⁴⁵ D. Fehlker,²³ L. Feldkamp,²⁸ D. Felea,⁸⁶ G. Feofilov,²⁴ A. Fernández Téllez,⁷³ A. Ferretti,⁴⁹ R. Ferretti,⁸⁴ J. Figiel,⁴⁴ M. A. S. Figueredo,⁷⁴ S. Filchagin,⁶⁷ D. Finogeev,⁹³ F. M. Fionda,²² E. M. Fiore,²² M. Floris,⁶ S. Foertsch,⁶⁸ P. Foka,²⁶ S. Fokin,¹⁵ E. Fragiaco,⁹⁴ M. Fragkiadakis,⁹⁵ U. Frankenfeld,²⁶ U. Fuchs,⁶ C. Furget,³⁴ M. Fusco Girard,⁸⁸ J. J. Gaardhøje,⁴⁶ M. Gagliardi,⁴⁹ A. Gago,⁷⁰ M. Gallio,⁴⁹ D. R. Gangadharan,²⁹ P. Ganoti,³⁶ C. Garabatos,²⁶ E. Garcia-Solis,⁹⁶ I. Garishvili,¹ J. Gerhard,²¹ M. Germain,³² C. Geuna,³⁹ A. Gheata,⁶ M. Gheata,⁶ B. Ghidini,²² P. Ghosh,¹⁰ P. Gianotti,⁵² M. R. Girard,⁹⁷ P. Giubellino,⁶ E. Gladysz-Dziadus,⁴⁴ P. Glässel,²⁷ R. Gomez,⁹⁸ E. G. Ferreira,³⁵ L. H. González-Trueba,⁹ P. González-Zamora,⁵⁶ S. Gorbunov,²¹ A. Goswami,⁹⁹ S. Gotovac,¹⁰⁰ V. Grabski,⁹ L. K. Graczykowski,⁹⁷ R. Grajcarek,²⁷ A. Grelli,⁵⁵ A. Grigoras,⁶ C. Grigoras,⁶ V. Grigoriev,⁵⁷ A. Grigoryan,¹⁰¹ S. Grigoryan,⁴⁵ B. Grinyov,¹⁹ N. Grion,⁹⁴ P. Gros,⁸⁰ J. F. Grosse-Oetringhaus,⁶ J.-Y. Grossiord,⁷⁸ R. Grosso,⁶ F. Guber,⁹³ R. Guernane,³⁴ C. Guerra Gutierrez,⁷⁰ B. Guerzoni,⁸ M. Guilbaud,⁷⁸ K. Gulbrandsen,⁴⁶ T. Gunji,¹⁰² A. Gupta,⁵¹ R. Gupta,⁵¹ H. Gutbrod,²⁶ Ø. Haaland,²³ C. Hadjidakis,⁶³ M. Haiduc,⁸⁶ H. Hamagaki,¹⁰² G. Hamar,⁷ B. H. Han,¹⁰³ L. D. Hanratty,⁴³ A. Hansen,⁴⁶ Z. Harmanova,⁵⁹ J. W. Harris,⁴ M. Hartig,³³ D. Hasegan,⁸⁶ D. Hatzifotiadou,¹⁷ A. Hayrapetyan,^{6,101} S. T. Heckel,³³ M. Heide,²⁸ H. Helstrup,²⁰ A. Herghelegiu,²⁵ G. Herrera Corral,⁷² N. Herrmann,²⁷ K. F. Hetland,²⁰ B. Hicks,⁴ P. T. Hille,⁴ B. Hippolyte,⁴⁷ T. Horaguchi,⁸¹ Y. Hori,¹⁰² P. Hristov,⁶ I. Hřivnáčová,⁶³ M. Huang,²³ S. Huber,²⁶ T. J. Humanic,²⁹ D. S. Hwang,¹⁰³ R. Ichou,¹² R. Ilkaev,⁶⁷ I. Ilkiv,⁹⁰ M. Inaba,⁸¹ E. Incani,⁷⁵ G. M. Innocenti,⁴⁹ P. G. Innocenti,⁶ M. Ippolitov,¹⁵ M. Irfan,¹¹ C. Ivan,²⁶ V. Ivanov,⁵⁰ A. Ivanov,²⁴ M. Ivanov,²⁶ O. Ivanytskyi,¹⁹ A. Jacholkowski,⁶ P. M. Jacobs,⁶⁴ L. Jancurová,⁴⁵ H. J. Jang,¹⁰⁴ S. Jangal,⁴⁷ M. A. Janik,⁹⁷ R. Janik,⁶⁶ P. H. S. Y. Jayarathna,⁴⁸ S. Jena,⁸⁷ R. T. Jimenez Bustamante,⁸⁵ L. Jirde,⁶ P. G. Jones,⁴³ H. Jung,¹³ A. Jusko,⁴³ A. B. Kaidalov,¹⁴ V. Kakoyan,¹⁰¹ S. Kalcher,²¹ P. Kaliňák,⁴⁰ M. Kalisky,²⁸ T. Kalliokoski,³⁷ A. Kalweit,¹⁰⁵ K. Kanaki,²³ J. H. Kang,⁷⁶ V. Kaplin,⁵⁷ A. Karasu Uysal,^{6,106} O. Karavichev,⁹³ T. Karavicheva,⁹³ E. Karpechev,⁹³ A. Kazantsev,¹⁵ U. Keschull,⁶² R. Keidel,¹⁰⁷ M. M. Khan,¹¹ S. A. Khan,¹⁰ P. Khan,⁶¹ A. Khanzadeev,⁵⁰ Y. Kharlov,⁵⁸ B. Kileng,²⁰ M. Kim,⁷⁶ J. S. Kim,¹³ D. J. Kim,³⁷ T. Kim,⁷⁶ B. Kim,⁷⁶ S. Kim,¹⁰³ S. H. Kim,¹³ D. W. Kim,¹³ J. H. Kim,¹⁰³ S. Kirsch,^{21,6} I. Kisel,²¹ S. Kiselev,¹⁴ A. Kisiel,^{6,97} J. L. Klay,¹⁰⁸ J. Klein,²⁷ C. Klein-Bösing,²⁸ M. Kliemant,³³ A. Kluge,⁶ M. L. Knichel,²⁶ A. G. Knospe,¹⁰⁹ K. Koch,²⁷ M. K. Köhler,²⁶ A. Kolojvari,²⁴ V. Kondratiev,²⁴ N. Kondratyeva,⁵⁷ A. Konevskikh,⁹³ A. Korneev,⁶⁷ C. Kottachchi Kankanamge Don,⁶⁰ R. Kour,⁴³ M. Kowalski,⁴⁴ S. Kox,³⁴ G. Koyithatta Meethaleveedu,⁸⁷ J. Kral,³⁷ I. Králik,⁴⁰ F. Kramer,³³ I. Kraus,²⁶ T. Krawutschke,^{27,110} M. Krelina,² M. Kretz,²¹ M. Krivda,^{43,40} F. Krizek,³⁷ M. Krus,² E. Kryshen,⁵⁰ M. Krzewicki,^{54,26} Y. Kucheriaev,¹⁵ C. Kuhn,⁴⁷ P. G. Kuijter,⁵⁴ P. Kurashvili,⁹⁰ A. Kurepin,⁹³ A. B. Kurepin,⁹³ A. Kuryakin,⁶⁷ S. Kushpil,³ V. Kushpil,³ H. Kvaerno,⁹² M. J. Kweon,²⁷ Y. Kwon,⁷⁶ P. Ladrón de Guevara,⁸⁵ I. Lakomov,^{63,24} R. Langoy,²³ C. Lara,⁶² A. Lardeux,³² P. La Rocca,⁴² C. Lazzeroni,⁴³ R. Lea,⁷¹ Y. Le Bornec,⁶³ S. C. Lee,¹³ K. S. Lee,¹³ F. Lefèvre,³² J. Lehnert,³³ L. Leistam,⁶ M. Lenhardt,³² V. Lenti,⁸⁹ H. León,⁹ I. León Monzón,⁹⁸ H. León Vargas,³³ P. Lévai,⁷ J. Lien,²³ R. Lietava,⁴³ S. Lindal,⁹² V. Lindenstruth,²¹ C. Lippmann,^{26,6} M. A. Lisa,²⁹ L. Liu,²³ P. I. Loenne,²³ V. R. Loggins,⁶⁰ V. Loginov,⁵⁷ S. Lohn,⁶ D. Lohner,²⁷ C. Loizides,⁶⁴ K. K. Loo,³⁷ X. Lopez,¹² E. López Torres,¹¹¹ G. Løvhøiden,⁹² X.-G. Lu,²⁷ P. Luettig,³³ M. Lunardon,⁵³ J. Luo,⁶⁹ G. Luparello,⁵⁵ L. Luquin,³² C. Luzzi,⁶ K. Ma,⁶⁹ R. Ma,⁴ D. M. Madagodahettige-Don,⁴⁸ A. Maevskaya,⁹³ M. Mager,^{105,6} D. P. Mahapatra,⁴¹ A. Maire,⁴⁷ M. Malaev,⁵⁰ I. Maldonado Cervantes,⁸⁵ L. Malinina,^{45,*} D. Mal'Kevich,¹⁴ P. Malzacher,²⁶ A. Mamonov,⁶⁷ L. Manceau,¹⁶ L. Mangotra,⁵¹ V. Manko,¹⁵ F. Manso,¹² V. Manzari,⁸⁹ Y. Mao,^{34,69} M. Marchisone,^{12,49} J. Mareš,¹¹² G. V. Margagliotti,^{71,94} A. Margotti,¹⁷ A. Marín,²⁶ C. A. Marin Tobon,⁶ C. Markert,¹⁰⁹ I. Martashvili,¹¹³ P. Martinengo,⁶ M. I. Martínez,⁷³ A. Martínez Davalos,⁹ G. Martínez García,³² Y. Martynov,¹⁹ A. Mas,³² S. Masciocchi,²⁶ M. Maserà,⁴⁹ A. Masoni,⁸³ L. Massacrier,^{78,32}

M. Mastromarco,⁸⁹ A. Mastroserio,^{22,6} Z. L. Matthews,⁴³ A. Matyja,^{44,32} D. Mayani,⁸⁵ C. Mayer,⁴⁴ J. Mazer,¹¹³ M. A. Mazzoni,⁹¹ F. Meddi,¹¹⁴ A. Menchaca-Rocha,⁹ J. Mercado Pérez,²⁷ M. Meres,⁶⁶ Y. Miake,⁸¹ L. Milano,⁴⁹ J. Milosevic,^{92,†} A. Mischke,⁵⁵ A. N. Mishra,⁹⁹ D. Miśkowiec,^{26,6} C. Mitu,⁸⁶ J. Mlynarz,⁶⁰ A. K. Mohanty,⁶ B. Mohanty,¹⁰ L. Molnar,⁶ L. Montaña Zetina,⁷² M. Monteno,¹⁶ E. Montes,⁵⁶ T. Moon,⁷⁶ M. Morando,⁵³ D. A. Moreira De Godoy,⁷⁴ S. Moretto,⁵³ A. Morsch,⁶ V. Muccifora,⁵² E. Mudnic,¹⁰⁰ S. Muhuri,¹⁰ H. Müller,⁶ M. G. Munhoz,⁷⁴ L. Musa,⁶ A. Musso,¹⁶ B. K. Nandi,⁸⁷ R. Nania,¹⁷ E. Nappi,⁸⁹ C. Nattrass,¹¹³ N. P. Naumov,⁶⁷ S. Navin,⁴³ T. K. Nayak,¹⁰ S. Nazarenko,⁶⁷ G. Nazarov,⁶⁷ A. Nedosekin,¹⁴ M. Nicassio,²² B. S. Nielsen,⁴⁶ T. Niida,⁸¹ S. Nikolaev,¹⁵ V. Nikolic,³⁰ V. Nikulin,⁵⁰ S. Nikulin,¹⁵ B. S. Nilsen,⁷⁷ M. S. Nilsson,⁹² F. Noferini,^{17,18} P. Nomokonov,⁴⁵ G. Nooren,⁵⁵ N. Novitzky,³⁷ A. Nyanin,¹⁵ A. Nyatha,⁸⁷ C. Nygaard,⁴⁶ J. Nystrand,²³ A. Ochirov,²⁴ H. Oeschler,^{105,6} S. K. Oh,¹³ S. Oh,⁴ J. Oleniacz,⁹⁷ C. Oppedisano,¹⁶ A. Ortiz Velasquez,^{80,85} G. Ortona,⁴⁹ A. Oskarsson,⁸⁰ P. Ostrowski,⁹⁷ J. Otwinowski,²⁶ K. Oyama,²⁷ K. Ozawa,¹⁰² Y. Pachmayer,²⁷ M. Pachr,² F. Padilla,⁴⁹ P. Pagano,⁸⁸ G. Paić,⁸⁵ F. Painke,²¹ C. Pajares,³⁵ S. K. Pal,¹⁰ S. Pal,³⁹ A. Palaha,⁴³ A. Palmeri,³⁸ V. Papikyan,¹⁰¹ G. S. Pappalardo,³⁸ W. J. Park,²⁶ A. Passfeld,²⁸ B. Pastirčák,⁴⁰ D. I. Patalakha,⁵⁸ V. Paticchio,⁸⁹ A. Pavlinov,⁶⁰ T. Pawlak,⁹⁷ T. Peitzmann,⁵⁵ E. Pereira De Oliveira Filho,⁷⁴ D. Peresunko,¹⁵ C. E. Pérez Lara,⁵⁴ E. Perez Lezama,⁸⁵ D. Perini,⁶ D. Perrino,²² W. Peryt,⁹⁷ A. Pesci,¹⁷ V. Peskov,^{6,85} Y. Pestov,¹¹⁵ V. Petráček,² M. Petran,² M. Petris,²⁵ P. Petrov,⁴³ M. Petrovici,²⁵ C. Petta,⁴² S. Piano,⁹⁴ A. Piccotti,¹⁶ M. Pikna,⁶⁶ P. Pillot,³² O. Pinazza,⁶ L. Pinsky,⁴⁸ N. Pitz,³³ F. Piuz,⁶ D. B. Piyarathna,⁴⁸ M. Płoskoń,⁶⁴ J. Pluta,⁹⁷ T. Pocheptsov,⁴⁵ S. Pochybova,⁷ P. L. M. Podesta-Lerma,⁹⁸ M. G. Poghosyan,^{6,49} K. Polák,¹¹² B. Polichtchouk,⁵⁸ A. Pop,²⁵ S. Porteboeuf-Houssais,¹² V. Pospíšil,² B. Potukuchi,⁵¹ S. K. Prasad,⁶⁰ R. Preghenella,^{17,18} F. Prino,¹⁶ C. A. Pruneau,⁶⁰ I. Pshenichnov,⁹³ S. Puchagin,⁶⁷ G. Puddu,⁷⁵ J. Pujol Teixido,⁶² A. Pulvirenti,^{42,6} V. Punin,⁶⁷ M. Putiš,⁵⁹ J. Putschke,^{60,4} E. Quercigh,⁶ H. Qvigstad,⁹² A. Rachevski,⁹⁴ A. Rademakers,⁶ S. Radomski,²⁷ T. S. Rähä,³⁷ J. Rak,³⁷ A. Rakotozafindrabe,³⁹ L. Ramello,⁸⁴ A. Ramírez Reyes,⁷² S. Raniwala,⁹⁹ R. Raniwala,⁹⁹ S. S. Räsänen,³⁷ B. T. Rascanu,³³ D. Rathee,⁵ K. F. Read,¹¹³ J. S. Real,³⁴ K. Redlich,^{90,116} P. Reichelt,³³ M. Reicher,⁵⁵ R. Renfordt,³³ A. R. Reolon,⁵² A. Reshetin,⁹³ F. Rettig,²¹ J.-P. Revol,⁶ K. Reygers,²⁷ L. Riccati,¹⁶ R. A. Ricci,¹¹⁷ T. Richert,⁸⁰ M. Richter,⁹² P. Riedler,⁶ W. Riegler,⁶ F. Riggi,^{42,38} M. Rodríguez Cahuantzi,⁷³ K. Røed,²³ D. Rohr,²¹ D. Röhrich,²³ R. Romita,²⁶ F. Ronchetti,⁵² P. Rosnet,¹² S. Rossegger,⁶ A. Rossi,⁵³ F. Roukoutakis,⁹⁵ C. Roy,⁴⁷ P. Roy,⁶¹ A. J. Rubio Montero,⁵⁶ R. Rui,⁷¹ E. Ryabinkin,¹⁵ A. Rybicki,⁴⁴ S. Sadovsky,⁵⁸ K. Šafařík,⁶ R. Sahoo,¹¹⁸ P. K. Sahu,⁴¹ J. Saini,¹⁰ H. Sakaguchi,¹¹⁹ S. Sakai,⁶⁴ D. Sakata,⁸¹ C. A. Salgado,³⁵ J. Salzwedel,²⁹ S. Sambyal,⁵¹ V. Samsonov,⁵⁰ X. Sanchez Castro,^{85,47} L. Šándor,⁴⁰ A. Sandoval,⁹ S. Sano,¹⁰² M. Sano,⁸¹ R. Santo,²⁸ R. Santoro,^{89,6} J. Sarkamo,³⁷ E. Scapparone,¹⁷ F. Scarlassara,⁵³ R. P. Scharenberg,⁶⁵ C. Schiaua,²⁵ R. Schicker,²⁷ H. R. Schmidt,^{26,120} C. Schmidt,²⁶ S. Schreiner,⁶ S. Schuchmann,³³ J. Schukraft,⁶ Y. Schutz,^{6,32} K. Schwarz,²⁶ K. Schweda,^{26,27} G. Scioli,⁸ E. Scomparin,¹⁶ P. A. Scott,⁴³ R. Scott,¹¹³ G. Segato,⁵³ I. Selyuzhenkov,²⁶ S. Senyukov,^{84,47} J. Seo,⁸² S. Serchi,⁷⁵ E. Serradilla,^{56,9} A. Sevcenco,⁸⁶ I. Sgura,⁸⁹ A. Shabetai,³² G. Shabratova,⁴⁵ R. Shahoyan,⁶ N. Sharma,⁵ S. Sharma,⁵¹ K. Shigaki,¹¹⁹ M. Shimomura,⁸¹ K. Shtejer,¹¹¹ Y. Sibiriak,¹⁵ M. Siciliano,⁴⁹ E. Sicking,⁶ S. Siddhanta,⁸³ T. Siemiarczuk,⁹⁰ D. Silvermyr,³⁶ c. Silvestre,³⁴ G. Simonetti,^{22,6} R. Singaraju,¹⁰ R. Singh,⁵¹ S. Singha,¹⁰ T. Sinha,⁶¹ B. C. Sinha,¹⁰ B. Sitar,⁶⁶ M. Sitta,⁸⁴ T. B. Skaali,⁹² K. Skjerdal,²³ R. Smakal,² N. Smirnov,⁴ R. J. M. Snellings,⁵⁵ C. Sjøgaard,⁴⁶ R. Soltz,¹ H. Son,¹⁰³ M. Song,⁷⁶ J. Song,⁸² C. Soos,⁶ F. Soramel,⁵³ I. Sputowska,⁴⁴ M. Spyropoulou-Stassinaki,⁹⁵ B. K. Srivastava,⁶⁵ J. Stachel,²⁷ I. Stan,⁸⁶ I. Stan,⁸⁶ G. Stefanek,⁹⁰ G. Stefanini,⁶ T. Steinbeck,²¹ M. Steinpreis,²⁹ E. Stenlund,⁸⁰ G. Steyn,⁶⁸ D. Stocco,³² M. Stolpovskiy,⁵⁸ K. Strabykin,⁶⁷ P. Strmen,⁶⁶ A. A. P. Suaide,⁷⁴ M. A. Subieta Vásquez,⁴⁹ T. Sugitate,¹¹⁹ C. Suire,⁶³ M. Sukhorukov,⁶⁷ R. Sultanov,¹⁴ M. Šumbera,³ T. Susa,³⁰ A. Szanto de Toledo,⁷⁴ I. Szarka,⁶⁶ A. Szostak,²³ C. Tagridis,⁹⁵ J. Takahashi,⁷⁹ J. D. Tapia Takaki,⁶³ A. Tauro,⁶ G. Tejada Muñoz,⁷³ A. Telesca,⁶ C. Terrevoli,²² J. Thäder,²⁶ D. Thomas,⁵⁵ R. Tieulent,⁷⁸ A. R. Timmins,⁴⁸ D. Tlusty,² A. Toia,^{21,6} H. Torii,^{119,102} L. Toscano,¹⁶ F. Tosello,¹⁶ D. Truesdale,²⁹ W. H. Trzaska,³⁷ T. Tsuji,¹⁰² A. Tumkin,⁶⁷ R. Turrisi,³¹ T. S. Tveter,⁹² J. Ulery,³³ K. Ullaland,²³ J. Ulrich,^{121,62} A. Uras,⁷⁸ J. Urbán,⁵⁹ G. M. Urciuoli,⁹¹ G. L. Usai,⁷⁵ M. Vajzer,^{2,3} M. Vala,^{45,40} L. Valencia Palomo,⁶³ S. Vallero,²⁷ N. van der Kolk,⁵⁴ P. Vande Vyvre,⁶ M. van Leeuwen,⁵⁵ L. Vannucci,¹¹⁷ A. Vargas,⁷³ R. Varma,⁸⁷ M. Vasileiou,⁹⁵ A. Vasiliev,¹⁵ V. Vechernin,²⁴ M. Veldhoen,⁵⁵ M. Venaruzzo,⁷¹ E. Vercellin,⁴⁹ S. Vergara,⁷³ D. C. Vernekohl,²⁸ R. Vernet,¹²² M. Verweij,⁵⁵ L. Vickovic,¹⁰⁰ G. Viesti,⁵³ O. Vikhlyantsev,⁶⁷ Z. Vilakazi,⁶⁸ O. Villalobos Baillie,⁴³ A. Vinogradov,¹⁵ Y. Vinogradov,⁶⁷ L. Vinogradov,²⁴ T. Virgili,⁸⁸ Y. P. Viyogi,¹⁰ A. Vodopyanov,⁴⁵ S. Voloshin,⁶⁰ K. Voloshin,¹⁴ G. Volpe,^{22,6} B. von Haller,⁶ D. Vranic,²⁶ G. Øvrebekk,²³ J. Vrláková,⁵⁹ B. Vulpescu,¹² A. Vyushin,⁶⁷ B. Wagner,²³ V. Wagner,² R. Wan,^{47,69} Y. Wang,²⁷ D. Wang,⁶⁹ Y. Wang,⁶⁹ M. Wang,⁶⁹ K. Watanabe,⁸¹

J. P. Wessels,^{6,28} U. Westerhoff,²⁸ J. Wiechula,¹²⁰ J. Wikne,⁹² M. Wilde,²⁸ G. Wilk,⁹⁰ A. Wilk,²⁸ M. C. S. Williams,¹⁷
 B. Windelband,²⁷ L. Xaplanteris Karampatsos,¹⁰⁹ H. Yang,³⁹ S. Yang,²³ S. Yasnopolskiy,¹⁵ J. Yi,⁸² Z. Yin,⁶⁹
 H. Yokoyama,⁸¹ I.-K. Yoo,⁸² J. Yoon,⁷⁶ W. Yu,³³ X. Yuan,⁶⁹ I. Yushmanov,¹⁵ C. Zach,² C. Zampolli,¹⁷
 S. Zaporozhets,⁴⁵ A. Zarochentsev,²⁴ P. Závada,¹¹² N. Zaviyalov,⁶⁷ H. Zbroszczyk,⁹⁷ P. Zelnicek,⁶² I. S. Zgura,⁸⁶
 M. Zhalov,⁵⁰ X. Zhang,^{12,69} D. Zhou,⁶⁹ Y. Zhou,⁵⁵ F. Zhou,⁶⁹ X. Zhu,⁶⁹ A. Zichichi,^{8,18} A. Zimmermann,²⁷
 G. Zinovjev,¹⁹ Y. Zoccarato,⁷⁸ and M. Zynovyev¹⁹

(ALICE Collaboration)

¹Lawrence Livermore National Laboratory, Livermore, California, United States

²Faculty of Nuclear Sciences and Physical Engineering, Czech Technical University in Prague, Prague, Czech Republic

³Nuclear Physics Institute, Academy of Sciences of the Czech Republic, Řež u Prahy, Czech Republic

⁴Yale University, New Haven, Connecticut, United States

⁵Physics Department, Panjab University, Chandigarh, India

⁶European Organization for Nuclear Research (CERN), Geneva, Switzerland

⁷KFKI Research Institute for Particle and Nuclear Physics, Hungarian Academy of Sciences, Budapest, Hungary

⁸Dipartimento di Fisica dell'Università and Sezione INFN, Bologna, Italy

⁹Instituto de Física, Universidad Nacional Autónoma de México, Mexico City, Mexico

¹⁰Variable Energy Cyclotron Centre, Kolkata, India

¹¹Department of Physics Aligarh Muslim University, Aligarh, India

¹²Laboratoire de Physique Corpusculaire (LPC), Clermont Université, Université Blaise Pascal, CNRS-IN2P3, Clermont-Ferrand, France

¹³Gangneung-Wonju National University, Gangneung, South Korea

¹⁴Institute for Theoretical and Experimental Physics, Moscow, Russia

¹⁵Russian Research Centre Kurchatov Institute, Moscow, Russia

¹⁶Sezione INFN, Turin, Italy

¹⁷Sezione INFN, Bologna, Italy

¹⁸Centro Fermi-Centro Studi e Ricerche e Museo Storico della Fisica "Enrico Fermi", Rome, Italy

¹⁹Bogolyubov Institute for Theoretical Physics, Kiev, Ukraine

²⁰Faculty of Engineering, Bergen University College, Bergen, Norway

²¹Frankfurt Institute for Advanced Studies, Johann Wolfgang Goethe-Universität Frankfurt, Frankfurt, Germany

²²Dipartimento Interateneo di Fisica 'M. Merlin' and Sezione INFN, Bari, Italy

²³Department of Physics and Technology, University of Bergen, Bergen, Norway

²⁴V. Fock Institute for Physics, St. Petersburg State University, St. Petersburg, Russia

²⁵National Institute for Physics and Nuclear Engineering, Bucharest, Romania

²⁶Research Division and ExtreMe Matter Institute EMMI, GSI Helmholtzzentrum für Schwerionenforschung, Darmstadt, Germany

²⁷Physikalisches Institut, Ruprecht-Karls-Universität Heidelberg, Heidelberg, Germany

²⁸Institut für Kernphysik, Westfälische Wilhelms-Universität Münster, Münster, Germany

²⁹Department of Physics, Ohio State University, Columbus, Ohio, United States

³⁰Rudjer Bošković Institute, Zagreb, Croatia

³¹Sezione INFN, Padova, Italy

³²SUBATECH, Ecole des Mines de Nantes, Université de Nantes, CNRS-IN2P3, Nantes, France

³³Institut für Kernphysik, Johann Wolfgang Goethe-Universität Frankfurt, Frankfurt, Germany

³⁴Laboratoire de Physique Subatomique et de Cosmologie (LPSC), Université Joseph Fourier, CNRS-IN2P3, Institut Polytechnique de Grenoble, Grenoble, France

³⁵Departamento de Física de Partículas and IGFAE, Universidad de Santiago de Compostela, Santiago de Compostela, Spain

³⁶Oak Ridge National Laboratory, Oak Ridge, Tennessee, United States

³⁷Helsinki Institute of Physics (HIP) and University of Jyväskylä, Jyväskylä, Finland

³⁸Sezione INFN, Catania, Italy

³⁹Commissariat à l'Énergie Atomique, IRFU, Saclay, France

⁴⁰Institute of Experimental Physics, Slovak Academy of Sciences, Košice, Slovakia

⁴¹Institute of Physics, Bhubaneswar, India

⁴²Dipartimento di Fisica e Astronomia dell'Università and Sezione INFN, Catania, Italy

⁴³School of Physics and Astronomy, University of Birmingham, Birmingham, United Kingdom

⁴⁴The Henryk Niewodniczanski Institute of Nuclear Physics, Polish Academy of Sciences, Cracow, Poland

⁴⁵Joint Institute for Nuclear Research (JINR), Dubna, Russia

⁴⁶Niels Bohr Institute, University of Copenhagen, Copenhagen, Denmark

⁴⁷Institut Pluridisciplinaire Hubert Curien (IPHC), Université de Strasbourg, CNRS-IN2P3, Strasbourg, France

⁴⁸University of Houston, Houston, Texas, United States

- ⁴⁹*Dipartimento di Fisica Sperimentale dell'Università and Sezione INFN, Turin, Italy*
⁵⁰*Petersburg Nuclear Physics Institute, Gatchina, Russia*
⁵¹*Physics Department, University of Jammu, Jammu, India*
⁵²*Laboratori Nazionali di Frascati, INFN, Frascati, Italy*
⁵³*Dipartimento di Fisica dell'Università and Sezione INFN, Padova, Italy*
⁵⁴*Nikhef, National Institute for Subatomic Physics, Amsterdam, Netherlands*
⁵⁵*Nikhef, National Institute for Subatomic Physics and Institute for Subatomic Physics of Utrecht University, Utrecht, Netherlands*
⁵⁶*Centro de Investigaciones Energéticas Medioambientales y Tecnológicas (CIEMAT), Madrid, Spain*
⁵⁷*Moscow Engineering Physics Institute, Moscow, Russia*
⁵⁸*Institute for High Energy Physics, Protvino, Russia*
⁵⁹*Faculty of Science, P.J. Šafárik University, Košice, Slovakia*
⁶⁰*Wayne State University, Detroit, Michigan, United States*
⁶¹*Saha Institute of Nuclear Physics, Kolkata, India*
⁶²*Institut für Informatik, Johann Wolfgang Goethe-Universität Frankfurt, Frankfurt, Germany*
⁶³*Institut de Physique Nucléaire d'Orsay (IPNO), Université Paris-Sud, CNRS-IN2P3, Orsay, France*
⁶⁴*Lawrence Berkeley National Laboratory, Berkeley, California, United States*
⁶⁵*Purdue University, West Lafayette, Indiana, United States*
⁶⁶*Faculty of Mathematics, Physics and Informatics, Comenius University, Bratislava, Slovakia*
⁶⁷*Russian Federal Nuclear Center (VNIIEF), Sarov, Russia*
⁶⁸*Physics Department, University of Cape Town, iThemba LABS, Cape Town, South Africa*
⁶⁹*Hua-Zhong Normal University, Wuhan, China*
⁷⁰*Sección Física, Departamento de Ciencias, Pontificia Universidad Católica del Perú, Lima, Peru*
⁷¹*Dipartimento di Fisica dell'Università and Sezione INFN, Trieste, Italy*
⁷²*Centro de Investigación y de Estudios Avanzados (CINVESTAV), Mexico City and Mérida, Mexico*
⁷³*Benemérita Universidad Autónoma de Puebla, Puebla, Mexico*
⁷⁴*Universidade de São Paulo (USP), São Paulo, Brazil*
⁷⁵*Dipartimento di Fisica dell'Università and Sezione INFN, Cagliari, Italy*
⁷⁶*Yonsei University, Seoul, South Korea*
⁷⁷*Physics Department, Creighton University, Omaha, Nebraska, United States*
⁷⁸*Université de Lyon, Université Lyon 1, CNRS/IN2P3, IPN-Lyon, Villeurbanne, France*
⁷⁹*Universidade Estadual de Campinas (UNICAMP), Campinas, Brazil*
⁸⁰*Division of Experimental High Energy Physics, University of Lund, Lund, Sweden*
⁸¹*University of Tsukuba, Tsukuba, Japan*
⁸²*Pusan National University, Pusan, South Korea*
⁸³*Sezione INFN, Cagliari, Italy*
⁸⁴*Dipartimento di Scienze e Tecnologie Avanzate dell'Università del Piemonte Orientale and Gruppo Collegato INFN, Alessandria, Italy*
⁸⁵*Instituto de Ciencias Nucleares, Universidad Nacional Autónoma de México, Mexico City, Mexico*
⁸⁶*Institute of Space Sciences (ISS), Bucharest, Romania*
⁸⁷*Indian Institute of Technology, Mumbai, India*
⁸⁸*Dipartimento di Fisica 'E.R. Caianiello' dell'Università and Gruppo Collegato INFN, Salerno, Italy*
⁸⁹*Sezione INFN, Bari, Italy*
⁹⁰*Soltan Institute for Nuclear Studies, Warsaw, Poland*
⁹¹*Sezione INFN, Rome, Italy*
⁹²*Department of Physics, University of Oslo, Oslo, Norway*
⁹³*Institute for Nuclear Research, Academy of Sciences, Moscow, Russia*
⁹⁴*Sezione INFN, Trieste, Italy*
⁹⁵*Physics Department, University of Athens, Athens, Greece*
⁹⁶*Chicago State University, Chicago, Illinois, United States*
⁹⁷*Warsaw University of Technology, Warsaw, Poland*
⁹⁸*Universidad Autónoma de Sinaloa, Culiacán, Mexico*
⁹⁹*Physics Department, University of Rajasthan, Jaipur, India*
¹⁰⁰*Technical University of Split FESB, Split, Croatia*
¹⁰¹*Yerevan Physics Institute, Yerevan, Armenia*
¹⁰²*University of Tokyo, Tokyo, Japan*
¹⁰³*Department of Physics, Sejong University, Seoul, South Korea*
¹⁰⁴*Korea Institute of Science and Technology Information, Daejeon, South Korea*
¹⁰⁵*Institut für Kernphysik, Technische Universität Darmstadt, Darmstadt, Germany*
¹⁰⁶*Yildiz Technical University, Istanbul, Turkey*
¹⁰⁷*Zentrum für Technologietransfer und Telekommunikation (ZTT), Fachhochschule Worms, Worms, Germany*
¹⁰⁸*California Polytechnic State University, San Luis Obispo, California, United States*

¹⁰⁹*The University of Texas at Austin, Physics Department, Austin, Texas, USA*

¹¹⁰*Fachhochschule Köln, Köln, Germany*

¹¹¹*Centro de Aplicaciones Tecnológicas y Desarrollo Nuclear (CEADEN), Havana, Cuba*

¹¹²*Institute of Physics, Academy of Sciences of the Czech Republic, Prague, Czech Republic*

¹¹³*University of Tennessee, Knoxville, Tennessee, United States*

¹¹⁴*Dipartimento di Fisica dell'Università "La Sapienza" and Sezione INFN, Rome, Italy*

¹¹⁵*Budker Institute for Nuclear Physics, Novosibirsk, Russia*

¹¹⁶*Institut of Theoretical Physics, University of Wrocław*

¹¹⁷*Laboratori Nazionali di Legnaro, INFN, Legnaro, Italy*

¹¹⁸*Indian Institute of Technology Indore (IIT), Indore, India*

¹¹⁹*Hiroshima University, Hiroshima, Japan*

¹²⁰*Eberhard Karls Universität Tübingen, Tübingen, Germany*

¹²¹*Kirchhoff-Institut für Physik, Ruprecht-Karls-Universität Heidelberg, Heidelberg, Germany*

¹²²*Centre de Calcul de l'IN2P3, Villeurbanne, France*

*Also at M. V. Lomonosov Moscow State University, D. V. Skobeltsyn Institute of Nuclear Physics, Moscow, Russia.

† Also at "Vinča" Institute of Nuclear Sciences, Belgrade, Serbia.